

Multiresolution Time Domain Based Different Wavelet Basis Studies of Scattering of Planar Stratified Medium and Rectangular Dielectric Cylinder

Qunsheng Cao and Kumar K. Tamma

AHPCRC, University of Minnesota, Minneapolis, MN 55415

Abstract – In this paper, several wavelet bases, namely, the Daubechies, the biorthogonal Coiflet, the Deslauriers-Dubuc interpolating functions, and the cubic spline Battle-Lemarie, are applied to the multiresolution time domain (MRTD) technique for planar stratified media and electromagnetic scattering. These MRTD schemes are studied via field expansions of the scaling functions in one-dimensional (1D) and two-dimensional (2D) cases. A rigorous treatment method for inhomogeneous media structures is given. We have focused here on the study of reflected and transmission coefficients for an electromagnetic wave propagation on a stratified slab media and the scattering width (SW) of a rectangular dielectric cylinder. The 1D propagation characteristics of single and periodical stratified media and the 2D scattering width of the MRTD schemes are compared with the results of the FDTD method. Finally, we describe the computational accuracy of the relative peaks and shifting position errors, via a comparison of the results of the MRTD scheme based on the different basis with those of the FDTD method.

Key words: Multiresolution Time Domain (MRTD) scheme; orthogonal and the biorthogonal wavelet bases; reflected and transmission coefficients and scattering width.

I. INTRODUCTION

In recent years, the multiresolution time-domain (MRTD) method [1]-[6] has been applied successfully to various electromagnetic field analyses. The fields of the MRTD scheme are first expanded as a summation of scaling functions and wavelet in space and rectangular pulse in time. Although many different orthogonal and bi-orthogonal families of wavelets in theory are available, there are a few fundamental requirements that restrict us to use the wavelet families: (i) Smoothness and differentiability, (ii) orthogonality, (iii) compact support, (iv) symmetry

or asymmetry, and (v) explicit analytic expression [7] in the choice of the scaling functions and wavelet in the Multiresolution Analysis (MRA) used in the MRTD scheme.

In application of the MRTD method, we can frequently choose and use different families of scaling functions and wavelets. The cubic spline Battle-Lemarié (BL) orthogonal wavelet family [8]-[9] is very desirable in the applications of the multiresolution time domain analysis. The Battle-Lemarié family of wavelets has good regularity and symmetry, the basis functions are orthogonal, and although the scaling functions and wavelet of BL don't have compact support, the functions decay exponentially. The Battle-Lemarié wavelet family was first introduced into the time-domain analysis for electromagnetic field applications [1], which is based on Galerkin's procedure of the method of moments (MOM) [10]; and later it progressed towards the introduction of the MRTD scheme in 1996 [1]. Another basis family used in the MRTD scheme is the Daubechies's compact support orthogonal wavelets [3], [7], and the family is with compact support and orthogonality, but they are far from being symmetric. The Daubechies's family is characterized as the one with an external phase and with the shortest support length for the given number of vanishing moments [7]. As a typical biorthogonal wavelet family, namely, the Cohen-Daubechies-Feauveau (CDF) wavelet family [5] used in the MRTD method, the CDF can be thought as a product of the marriage between the spline family and Daubechies' construction. The CDF spline family is therefore indexed by the pair (n, \hat{n}) and denoted by CDF (n, \hat{n}) , n is order of B-spline function and \hat{n} is the vanishing moments of the wavelet. Yet another wavelet basis used in the MRTD scheme, the spline biorthogonal Coiflet wavelets family, a variation of the Daubechies family [6], is with almost symmetric properties, orthonormal and compactly supported on limited intervals. The MRTD schemes also adopt the Deslauriers-Dubuc

interpolating wavelets family [4], and the Haar wavelet family [6] as field expansion basis. The MRTD schemes based on these different wavelet bases have shown a good potential to approximate the exact solutions. For example, the cubic spline Battle-Lemarie scaling and wavelet basis, which is the first wavelet basis used in the MRTD scheme, can even be obtained near Nyquist sampling limit in using the Galerkin's sampling procedure with high computing accuracy [1]. In the MRTD scheme a reduction of grid density is inherent in the computations; however, there is a need to ensure adequate computing accuracy compared with the traditional finite difference time domain (FDTD) method. We note that different wavelet basis used in the MRTD schemes, because of the different wavelet bases; they have different properties of the compact support, and decay exponentially with symmetry. Therefore, there exist varied indexes of summation in the field expansions and for convergence for the different basis, which leads to some differences in computing accuracy for practical structures.

In this paper, we present exact algorithms of the MRTD scheme based on different wavelet basis, and the functions of field expansion are chosen as the scaling functions of the various wavelet bases in one-dimension (1D) and two-dimensions (2D), respectively. We provide the expansion functions of a different wavelet family, and give the exact formulations of the dielectric regions of the MRTD for an inhomogeneous lossless media. Finally, we calculate the wave reflected and transmission coefficients in the 1D, and the scattered width (SW) of a rectangular dielectric cylinder in the 2D case, respectively. We also compare the computing accuracies of the MRTD scheme based on the different wavelet bases with those of the FDTD method, and discuss the implementation aspects and approximations that are employed in providing simplification of the formulations.

II. FORMULATION AND WAVELET BASES CHOSEN

Firstly, we consider a 2D scattering analysis of an inhomogeneous lossless medium with the permittivity ϵ_r . For the MRTD scheme, we adopt a pure scattered-field formulation employed in the

FDTD technique [11], in which the incident field \vec{E}^{inc} is added only to the targets to describe time-domain electromagnetic fields. The Maxwell's equations for 2D TM_z mode can be written as

$$\frac{\partial H_x^{scat}}{\partial t} = -\frac{1}{\mu_0} \frac{\partial E_z^{scat}}{\partial y} \quad (1)$$

$$\frac{\partial H_y^{scat}}{\partial t} = \frac{1}{\mu_0} \frac{\partial E_z^{scat}}{\partial x} \quad (2)$$

$$\epsilon_0 \epsilon_r \frac{\partial E_z^{scat}}{\partial t} = -\epsilon_0 (\epsilon_r - 1) \frac{\partial E_z^{inc}}{\partial t} + \left(\frac{\partial H_y^{scat}}{\partial x} - \frac{\partial H_x^{scat}}{\partial y} \right) \quad (3)$$

where E^{scat} indicates the scattered E -field. The relative permittivity ϵ_r is given as

$$\epsilon_r(x, y) = \begin{cases} \epsilon_r^\kappa, & \text{for } x_1^\kappa \leq x \leq x_2^\kappa, y_1^\kappa \leq y \leq y_2^\kappa \\ 1, & \text{elsewhere} \end{cases} \quad (\kappa = 0, 1, 2, \dots, N) \quad (4)$$

where N is the total number of participating media, x_1^κ (y_1^κ) and x_2^κ (y_2^κ) are the x (y)-coordinates of lower and upper limits of the κ -th dielectric medium. Next, the field values are expanded as separable combination for the orthogonal scaling functions $\phi(\xi)$, ($\xi = x, y$) in space, and the Haar functions (rectangular pulse) $h(t)$ in time, respectively. For example, the scattering fields are expanded as

$$H_x^{scat}(x, y, t) = \sum_{n,i,j=-\infty}^{+\infty} \phi_x H_{i,j+\frac{1}{2}}^n \tilde{\phi}_i(x) \tilde{\phi}_{j+\frac{1}{2}}(y) h_n(t) \quad (5)$$

$$H_y^{scat}(x, y, t) = \sum_{n,i,j=-\infty}^{+\infty} \phi_y H_{i+\frac{1}{2},j}^n \tilde{\phi}_{i+\frac{1}{2}}(x) \tilde{\phi}_j(y) h_n(t) \quad (6)$$

$$E_z^{scat}(x, y, t) = \sum_{n,i,j=-\infty}^{+\infty} E_{i,j}^n \tilde{\phi}_i(x) \tilde{\phi}_j(y) h_n(t). \quad (7)$$

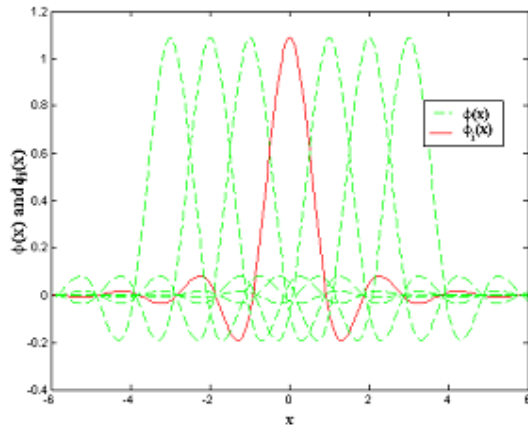
where $\tilde{\phi}_i(\xi)$ denotes dual scaling shifted by i units. Similarly, the expansion forms of the incident field are similar with that of the scattering field. The functions $h_n(t)$ and $\phi_i(\xi)$ or $\tilde{\phi}_i(\xi)$ are generated from the basic functions by dilation and translation as

$$h_n(t) = h\left(\frac{t}{\Delta t} - n + \frac{1}{2}\right) \quad (8)$$

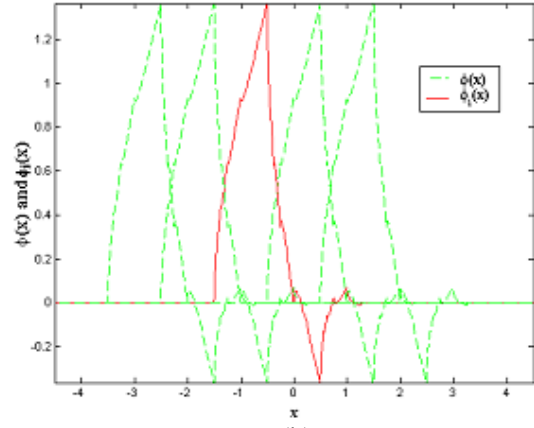
and

$$\phi_i(\xi) = \phi\left(\frac{\xi}{\Delta\xi} - i\right) \text{ or } \tilde{\phi}_i(\xi) = \tilde{\phi}\left(\frac{\xi}{\Delta\xi} - i\right). \quad (9)$$

If the scaling function $\phi_i(\xi) = \tilde{\phi}_i(\xi)$, then the expansion is called an orthogonal expansion, otherwise it is called a biorthogonal expansion. In this paper, we have considered a variety of different scaling functions $\phi(\xi)$ and its shifted functions $\phi_i(\xi)$ (or shifted dual functions $\tilde{\phi}_i(\xi)$), that is, the cubic spline Battle-Lemarie scaling function, the compact support Daubechies scaling function D_4 ($p=2$) [12], the compact support spline biorthogonal (Coiflet wavelet) scaling function ($p=2, \tilde{p}=2$) [13], the compact support spline biorthogonal (Coiflet wavelet) scaling function ($p=4, \tilde{p}=4$) [13], and the Deslauriers-Dubuc interpolating functions [14] as a scaling function, respectively. As examples, Figs. 1 give the distributions of the cubic spline Battle-Lemarie scaling function and Daubechies scaling function D_4 , and their corresponding shift functions. In particular, the Deslauriers-Dubuc scaling function has its dual scaling function, where the dual function can be chosen as the Dirac delta function: $\tilde{\phi}(\xi) = \delta(\xi)$ [14]-[16], and the interpolating scaling function constructed as the autocorrelation function of the Daubechies' orthogonal scaling function with $N=2$ [14]-[16].



(a)



(b)

Fig. 1. The scaling function $\phi(x)$ and its shifted functions $\phi_i(x)$ (or dual shifted functions $\tilde{\phi}_i(x)$). (a) The cubic spline Battle-Lemarie basis, and (b) the Daubechies D_4 basis.

Substitution of the field expansions into the Maxwell equations (1)-(3), and then sampled using the basis function as the test function by the standard a Galerkin's procedure leads to the following two update equations of the H -fields:

$$\begin{aligned} \text{scat}_{\phi x} H_{i,j+\frac{1}{2}}^{n+\frac{1}{2}} &= \text{scat}_{\phi x} H_{i,j+\frac{1}{2}}^{n-\frac{1}{2}} \\ &- \frac{1}{\mu_0} \sum_{\nu} a(\nu) \text{scat}_{\phi z} E_{i,j+\nu+\frac{1}{2}}^n \frac{\Delta t}{\Delta y} \end{aligned} \quad (10a)$$

$$\begin{aligned} \text{scat}_{\phi y} H_{i+\frac{1}{2},j}^{n+\frac{1}{2}} &= \text{scat}_{\phi y} H_{i+\frac{1}{2},j}^{n-\frac{1}{2}} \\ &- \frac{1}{\mu_0} \sum_{\nu} a(\nu) \text{scat}_{\phi z} E_{i+\nu+\frac{1}{2},j}^n \frac{\Delta t}{\Delta x}. \end{aligned} \quad (10b)$$

Table I. Connection coefficients $\alpha(\nu)$,

$$(\alpha(-\nu) = -\alpha(\nu-1))$$

ν	Daubechies	Coiflet ($p=2, \tilde{p}=2$)	Coiflet ($p=4, \tilde{p}=4$)
0	1.22953239	1.23464519	1.31103170
1	-0.09358996	-0.09715386	-0.15600966
2	0.01025133	0.01162914	0.04199606
3	0.00003558	-0.00019002	-0.00865439
4			0.00083094

The coefficients $\alpha(\nu)$ connecting the scaling and their derivative functions are obtained by a numerical integral method in the Fourier domain [1] and Table I lists the coefficients $\alpha(\nu)$ of the Daubechies D_4 and biorthogonal Coiflet scaling functions.

The derivation of the update equation for the E fields is quite involved, since all orthogonal relations of the bases functions are not valid due to the introduction of the inhomogeneous region. Starting from the time domain equation (3), we derive the following update equation for the E field:

$$\begin{aligned} \frac{scat}{\phi_z} E_{i,j}^{n+1} = & \frac{scat}{\phi_z} E_{i,j}^n + \frac{1}{\left[1 + \sum_{\kappa=1}^N (\epsilon_r^\kappa - 1) \alpha_{i,i}^\kappa \beta_{j,j}^\kappa\right]} \times \\ & \sum_{i'=i-\Lambda}^{i'+\Lambda} \sum_{j'=j-\Lambda}^{j'+\Lambda} \sum_{\kappa=1}^N (\epsilon_r^\kappa - 1) \alpha_{i,i'}^\kappa \beta_{j,j'}^\kappa \left(\frac{inc}{\phi_z} E_{i',j'}^{n+1} - \frac{inc}{\phi_z} E_{i',j'}^n \right) \\ & + \frac{1}{\epsilon_0 \left[1 + \sum_{\kappa=1}^N (\epsilon_r^\kappa - 1) \alpha_{i,i}^\kappa \beta_{j,j}^\kappa\right]} \times \\ & \sum_{\nu} a(\nu) \left(\frac{scat}{\phi_y} H_{i+\nu+1/2,j}^{n+1/2} \frac{\Delta t}{\Delta x} - \frac{scat}{\phi_x} H_{i,j+\nu+1/2}^{n+1/2} \frac{\Delta t}{\Delta y} \right) \end{aligned} \quad (11)$$

and the coefficients $\alpha_{i,i'}^\kappa$ and $\beta_{j,j'}^\kappa$ are defined as:

$$\alpha_{i,i'}^\kappa = \frac{1}{\Delta x} \int_{x_1^\kappa}^{x_2^\kappa} \phi_{i'}(x) \tilde{\phi}_i(x) dx \quad (12a)$$

$$\beta_{j,j'}^\kappa = \frac{1}{\Delta y} \int_{y_1^\kappa}^{y_2^\kappa} \phi_{j'}(y) \tilde{\phi}_j(y) dy \quad (12b)$$

where (x_1^κ, x_2^κ) and (y_1^κ, y_2^κ) are the lower and upper limits of the κ -th dielectric medium along the x - and y -directions, respectively. N is the number of dielectric media in the computational domain, and Λ is an adjustable constant, which is determined by the size of stencil effect, the computing accuracy requirement and the localization property of the scaling functions. Usually the constant Λ is chosen as 6 to 9 for the cubic spline Battle-Lemarie wavelet basis, and 4 to 6 for the Daubechies D_4 and Biorthogonal Coiflet basis. Equation (11) indicates that for the κ -th

scattering target, the distribution of E -field has relation with that of the fields within an extended region, which is covered by the region: $\left[(i_2^k + \Lambda) - (i_1^k - \Lambda), (j_2^k + \Lambda) - (j_1^k - \Lambda) \right]$.

In the derivation process we have used the main diagonal approximation in the evaluation, *i.e.*, we replace $\alpha_{i,i'}^\kappa \beta_{j,j'}^\kappa$ by $\alpha_{i,i'}^\kappa \beta_{j,j'}^\kappa \delta_{i,i'} \delta_{j,j'}$. This approximation is justified because of the compact support of the bases functions and the fact that the main diagonal coefficients are larger than those of the non-diagonal coefficients [17].

Equation (12) involves the scaling and its dual functions and the products of them. From these multiplicative products of functions $\phi(x) \tilde{\phi}_i(x)$ of the different wavelet bases we can obtain roughly the extended dielectric region for different wavelet bases, that is, we can estimate an adjustable value Λ according to different accuracy requirements.

Now we consider one-dimensional wave propagation TEM mode. Considering the constitutive relation for the E -field, $D_y = \epsilon E_y$, we derive the update equation of the E -field in the dielectric region, that is,

$$\phi_y D_i^{n+1} = \phi_y D_i^n - \sum_{\nu=-\infty}^{+\infty} a(\nu) \frac{scat}{\phi_z} H_{i+\nu+1/2}^{n+1/2} \frac{\Delta t}{\Delta x} \quad (13)$$

$$\begin{aligned} \frac{\phi_y D_i^n}{\epsilon_0} = & \sum_{i'=-\infty}^{+\infty} \phi_y E_{i'}^n \left(\delta_{i,i'} + \sum_{k=0}^N (\epsilon_r^k - 1) \alpha_{i,i'}^k \right) \\ \approx & \phi_y E_i^n + \sum_{i'=i-\Lambda}^{i+\Lambda} \sum_{k=0}^N (\epsilon_r^k - 1) \alpha_{i,i'}^k \phi_y E_{i'}^n. \end{aligned} \quad (14)$$

Employing an inverse matrix technique, equation (14) can be re-written as a typical update equation as given by

$$\phi_y E_i^n = \frac{1}{\epsilon_0} \sum_{k=1}^N \sum_{i'=i-\Lambda}^{i'+\Lambda} \left(\chi^k \right)_{i,j} \phi_y D_j^n \quad (15)$$

where

$$\left[\chi^k \right] = \left[I + \sum_{i'=i-\Lambda}^{i'+\Lambda} (\epsilon_r^k - 1) \alpha_{i,i'}^k \right]^{-1}. \quad (16)$$

Numerically, for the MRTD solver we can pre-calculate the coefficients $\alpha_{i,i'}^k$, $\beta_{j,j'}^k$ and dielectric matrix $[\chi]$, and can pre-store them at the start of

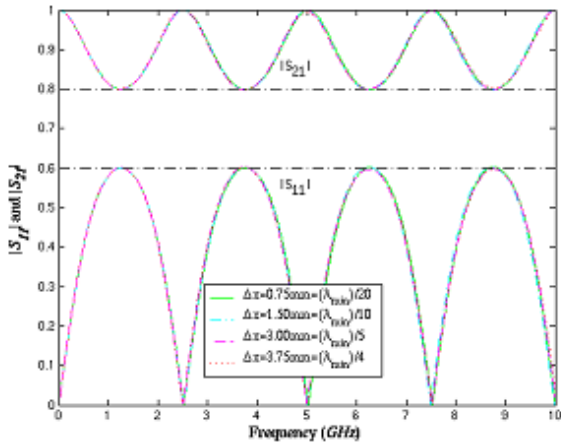
the MRTD code. Due to the requirement of a square matrix, the dimensions of the connected dielectric matrix $[\chi]$ in (16) are $(i_2^k - i_2^k + 2\Lambda) \times (i_2^k - i_2^k + 2\Lambda)$ for each dielectric region. As an approximation, we can only consider the main diagonal element in (16) as explained previously; and as a further approximation we can reduce the dielectric region to a real dielectric region, and make the dielectric width equal to the slab width by decreasing $\Lambda \rightarrow 0$.

III. NUMERICAL RESULTS

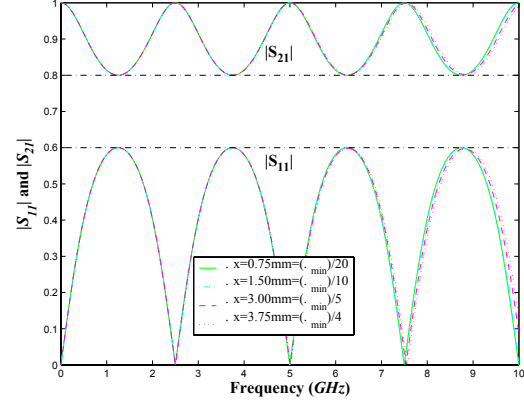
As a first example, we consider a *TEM* plane transient pulse with a maximum frequency $f_{\max} = 10\text{GHz}$, generated by an exciting E_y field that is incident on a dielectric slab characterized with a relative permittivity $\epsilon_r = 4$, and the width is $3 \times 10^{-2} m$ and $\Delta t = 1.25 \times 10^{-12} s$. The computational domain and the grid configuration are listed in Table II, in which NX is the total computing dimension, i_1, i_2 are the slab positions, and i_{r1}, i_{r2} are the record positions for the reflected and transmission wave, respectively.

Table II. Configuration of dielectric slab

NX (cell)	i_1 (cell)	i_2 (cell)	i_{r1} (cell)	i_{r2} (cell)
300	140	170	120	200
150	70	90	60	100
75	35	45	30	50
60	28	36	24	40



(a)



(b)

Fig. 2. Magnitudes of reflection coefficient S_{11} and transmission coefficient S_{21} versus frequency in a single-layer dielectric slab system. (a) the cubic spline Battle-Lemarie basis, and (b) the Daubechies D_4 basis.

Figures 2 show the results of the reflected and transmission coefficients for one dielectric slab for the cubic spline Battle-Lemarie wavelet basis and the Daubechies wavelet basis, respectively. In order to compare the computing accuracy for different wavelet bases, we have to define two relative errors. One is the relative peak error

$$\Sigma_p = \frac{R_{analysis}(n) - R_{MRTD}(n)}{R_{analysis}(n)},$$

which is involved

with the value change of the reflected coefficient curve at a specified peak position, where $R(n)$ is the corresponding value of the reflected coefficient at the n -th peak in the reflected coefficient curves. The other one is the relative shifting error

$$\Sigma_s = \frac{f_0 - f_{MRTD}}{f_0},$$

which is involved the

frequency position shifting changes along the horizontal axis in the coefficients curves, where f_0 is a corresponding frequency value of the analytical solution along the horizontal axis.

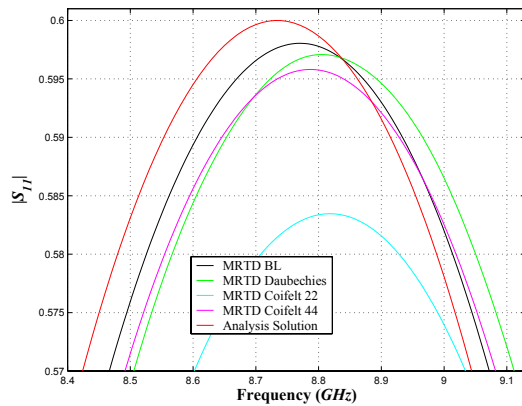
In Table III are given the relative peak errors Σ_p corresponding to the third peak, and the relative shifting error Σ_s corresponds to the frequency value along the horizontal position

$f_0 = 9.98\text{GHz}$ for the different MRTD wavelet basis compared with the analytical solution with increasing cell unit Δx . From Figs. 2 and Table III, it is found that the reflected and transmission coefficients of the MRTD scheme based on the cubic spline Battle-Lemarie wavelet are of reasonable accuracy and within the limits of the computational relative peak error and the relative shifting error.

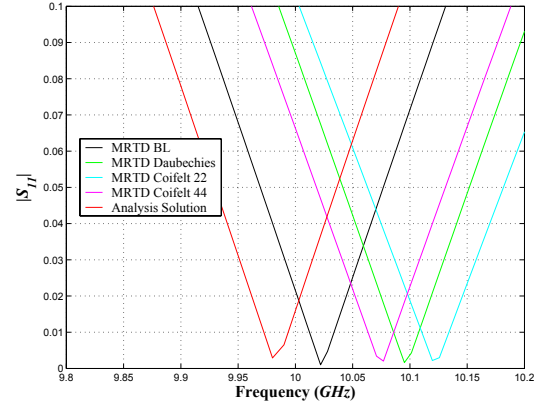
Figures 3(a) and 3(b) show the enlarged local peak portion of the reflected coefficient curve and the enlarged local horizontal portion that correspond to the third peak and the frequency value along the horizontal position with the frequency value of the analytical solution $f_0 = 9.98\text{GHz}$ with $\Delta x = \lambda_{\min}/5$, respectively.

Table III. Relative peak error at the third peak and shifting position error of the reflected coefficients at $f = 9.98\text{GHz}$

Δx (mm)	Battle-Lemarie (%)		Daubechies (%)		Coifelt ($p=2, \tilde{p}=2$) (%)		Coifelt ($p=4, \tilde{p}=4$) (%)	
	Σ_f	Σ_s	Σ_f	Σ_s	Σ_f	Σ_s	Σ_f	Σ_s
0.75	-0.37	-0.29	-0.17	-0.18	0.02	-0.18	0.02	-0.18
1.50	-0.33	-0.12	0.02	-0.29	0.17	-0.29	-0.02	-0.18
3.00	0.32	-0.42	0.48	-1.14	2.75	-1.40	0.70	-0.98
3.75	0.35	-0.72	0.57	-1.70	6.47	-2.18	2.30	-2.25



(a)



(b)

Fig. 3. Enlarged magnitudes of the reflection coefficients S_{11} versus frequency in a single-layer dielectric slab system. (a) at the third peak position, (b) at the 10GHz frequency position with cell size $\Delta x = \lambda_{\min}/5$.

For the reflected coefficients obtained with only the main diagonal elements in the dielectric matrix, that is, the matrix elements that only correspond to the same units as α_{ii}^k , the Daubechies D_4 scaling basis, the reflected coefficients show a smaller computational relative peak error and smaller relative shifting position error than that of the other bases for the ‘coarse’ cell size. Therefore, as a simplification of the main diagonal approximation, the Daubechies D_4 scaling basis can be chosen as a basic basis to be used in the MRTD expansion.

Figure 4 give the reflected coefficients of a periodical dielectric stratified 10 layer media using the MRTD scheme based on the Battle-Lemarie scaling functions; the width of the slab is $w_1 = 3 \times 10^{-2} m$, the width between slabs is $w_2 = 3 \times 10^{-2} m$, and the values are compared with the analytic solution. It can be seen that the MRTD scheme exhibits high computing accuracy and larger savings in computing memory, and nearly the same computing time compared with the FDTD method for a complicated periodic structure. The total lengths of the periodic slabs are $NX = 1020$ for the FDTD and $NX = 204$ for

the MRTD. The CPU time is about 92.5 seconds for the FDTD with $\Delta x = \lambda_{\min}/20$, about 107.2 seconds for the MRTD based on Battle-Lemarie scaling functions with $\Delta x = \lambda_{\min}/4$, and about 110 seconds for the MRTD based on the Daubechines D_4 scaling functions with $\Delta x = \lambda_{\min}/4$. A total of 40,000 time steps were used for the same 500 MHz Pentium III (Katmai) computations.

Next, we investigate the scattering width (SW), σ_s , for a square dielectric cylinder with a plane wave incident with a maximum frequency of $f_{\max} = 5\text{GHz}$. The dimension of the target is $0.18 \times 0.18\text{m}^2$ with the relative permittivity $\epsilon_r = 4$, and the discretization employs $\Delta t = 2.5 \times 10^{-12}\text{s}$, and the total number of steps is 4000 for the MRTD scheme and the FDTD method. Ten layers of the APL boundary are used. In Fig. 5 is plotted the SW of the MRTD scheme based on different wavelet bases with that of the FDTD method for the TM_z mode. The results of the MRTD scheme are in good agreement with that of the FDTD for a specified frequency at a specified incident and scattering angle. However, the computational space for the MRTD scheme is $60\Delta x \times 60\Delta y$, and is only about 14.1% of that employed in the FDTD, which is given by $160\Delta x \times 160\Delta y$.

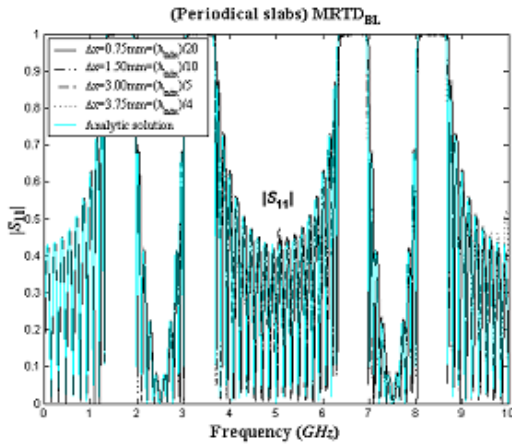


Fig. 4. Magnitudes of the reflection coefficients S_{11} are for a periodical dielectric stratified ten layer media by the cubic spline Battle-Lemarie wavelet basis.

In order to compare the accuracies of scattered width of the MRTD scheme based on different wavelet basis, we again employ the concept of the relative peak error $\Sigma_p = \frac{\sigma_{FDTD}(n) - \sigma_{MRTD}(n)}{\sigma_{FDTD}(n)}$,

where $\sigma(n)$ is the value of SW at the specified n -th peak in the scatter width curve, and the relative shifting position error $\Sigma_s = \frac{f_0 - f_{MRTD}}{f_0}$, where

f_0 and f_{MRTD} are corresponding frequency values of the FDTD method and the MRTD scheme in the horizontal axis for the n -th peak in the SW curve, respectively.

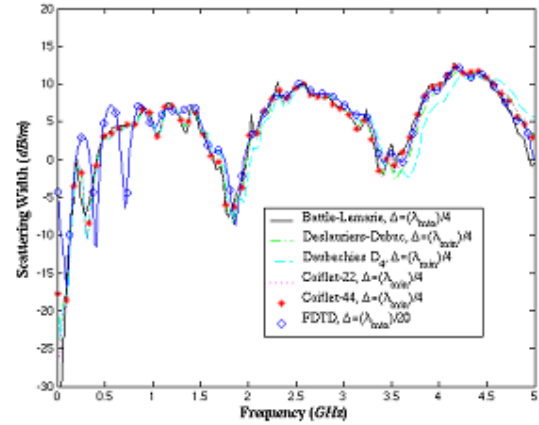


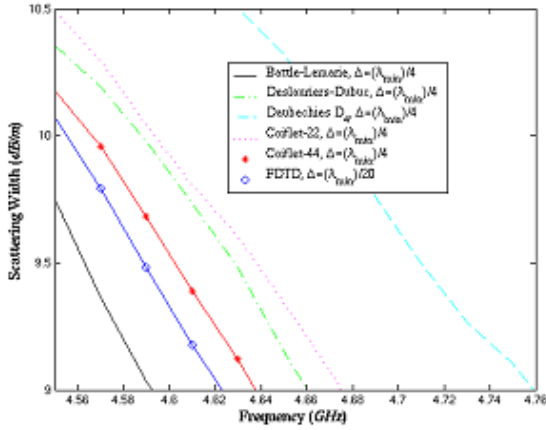
Fig. 5. Magnitudes of the scattering widths as a function of frequency ($\phi_i = 30^\circ$, $\phi_s = 30^\circ$) for the different wavelet bases and FDTD method are for a TM_z wave incident on a square dielectric cylinder, where ϕ_i and ϕ_s are the incident and scattering angles of the wave, respectively.

Table IV lists the two relative errors, in which the relative peak errors are for the third curve peak and shifting position errors are for the specified frequency value along the horizontal position. For example, for the FDTD method the value of frequency along the horizontal position is about $f_0 = 4.646\text{GHz}$.

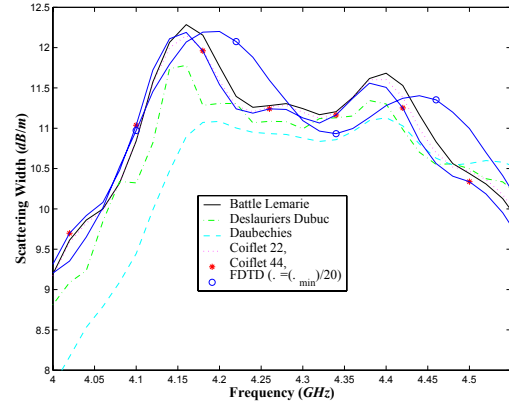
Table IV. Relative peak and shifting position errors of the scattered width for the third peak curve

Δx (mm)	Battle-Lemarie (%)		Daubechies (%)		Coiflet ($p=2, \tilde{p}=2$) (%)		Coiflet ($p=4, \tilde{p}=4$) (%)		Deslauriers -Dubuc (%)	
	Σ_f	Σ_s	Σ_f	Σ_s	Σ_f	Σ_s	Σ_f	Σ_s	Σ_f	Σ_s
1.00	-1.88	0.78	13.11	1.92	3.28	1.02	3.69	-3.22	5.98	-0.26
0.75	-1.00	0.73	10.49	2.90	2.05	1.01	-0.33	-0.30	4.92	-0.74
0.50	-0.57	0.39	9.18	-1.02	0.41	0.17	-1.97	0.56	3.44	-0.04

A careful study of the SW with varied cell sizes of different MRTD wavelet bases and from Table IV, we find that the scattering widths of the cubic spline Battle-Lemarie wavelet basis have reasonable accuracy within the limits of the computational relative error, and higher accuracy than that of other wavelet bases relative to the results of the FDTD method with different cell sizes. Figs. 6(a) and (b) are the enlarged scattered width curves corresponding to different wavelet bases with the cell size $\Delta l = \lambda_{\max}/6$. From Figs. 6(a)-(b) and Table IV, the results of the Daubechies D4 basis show a larger peak and shifting position errors than that of the other wavelet bases.



(a)



(b)

Fig. 6. Enlarged scattering widths as a function of frequency ($\phi_t=30^\circ$, $\phi_s=30^\circ$) for different cell sizes are for a TM_z wave incident on a square dielectric cylinder. (a) at the third peak position (b) at the 5.0GHz frequency position with cellsize $\Delta = 0.75 \times 10^{-2} m = \lambda_{\max}/4$.

IV. CONCLUSIONS

In this paper, a multiresolution time domain scheme based on different wavelet bases have been explored, and have been applied to electromagnetic analysis of a 1D wave with reflected and transmission, and a 2D scattering problem in an inhomogeneous dielectric region. The formulations of the update equations of the E -field were derived. We have calculated the reflected, transmitting coefficients, and the scattered width in 1D and 2D for the MRTD schemes, respectively, corresponding to different wavelet bases. The computed results have been compared with those derived from the FDTD and analytical solutions. We have also estimated the values of the relative peak errors and the shifting position errors at a specified horizontal frequency for the different MRTD schemes. The different MRTD wavelet schemes show the comparative accuracies of the different wavelet bases at specified frequency and peak positions.

ACKNOWLEDGMENT

The authors are very pleased to acknowledge support by the Army High Performance Computing Research Center (AHPCRC) under the auspices of Department of the Army, Army Research Laboratory (ARL) under contact number DAAD19-01-2-0014. Dr. Raju Namburu is the technical monitor. The content does not necessarily reflect the position or policy of government, and no official endorsement should be inferred. Other related support in form of computer grants from the Minnesota Supercomputer Institute (MSI), Minneapolis, Minnesota is also gratefully acknowledged.

REFERENCES

- [1] M. Krumpholz and L.P.B. Katehi, "MRTD: New time domain schemes based on multiresolution analysis," *IEEE Trans. Microwave Theory Tech.*, vol. 44, no. 4, pp. 555-571, April 1996.
- [2] Q. Cao, Y. Chen and R. Mittra, "Multiple image technique (MIT) and anisotropic perfectly matched layer (APML) in implementation of MRTD scheme for boundary truncations of microwave structures," *IEEE Trans. Microwave Theory Tech.*, vol. 50, no. 6, pp. 1578-1589, June 2002.
- [3] Y. W. Cheong, Y. M. Lee, K. H. Ra, J. G. Kang and C. C. Shin, "Wavelet-Galerkin scheme of time-dependent inhomogeneous electromagnetic problem," *IEEE Microwave Guide Lett.*, vol. 9, no. 8, p. 297-299, Aug. 1999.
- [4] M. Fujii and W.J.R. Hoefer, "A wavelet formulation of the finite-difference method: full-vector analysis of optical waveguide junctions," *IEEE J. Quantum electron.*, vol. 37, no. 8, Aug. 2001.
- [5] T. Dogaru and L. Carin, "Multiresolution time-domain algorithm using CDF biorthogonal wavelet," *IEEE Trans. Microwave Theory Tech.*, vol. 49, no. 5, pp. 902-912, May 2001.
- [6] M. Fujii and W. J. R. Hoefer, "A three-dimensional Haar-wavelet-based multiresolution analysis similar to the FDTD method Derivation and application," *IEEE Trans. Microwave TheoryTech.*, vol. 46, pp. 2463-2475, Dec. 1998.
- [7] I. Daubechies, *Ten Lectures on Wavelets*. Philadelphia, PA: SIAM, 1992.
- [8] G. Battle, "A block spin construction of ondelettes. Part I: Lemarié," *Commun. Math. Phys.*, vol. 110, pp. 601-615, 1987.
- [9] P. G. Lemarié, "Ondelettes à localization exponentielles," *J. Math. Pures et appl.*,
- [10] J. J H. Wang, *Generalized Moment Methods in Electromagnetic: Formulation and Computer Solution of Integral Equations*. New York: Wiley Interscience, 1991.
- [11] K. S. Kunz and R.J. Luebbers, *The finite difference time domain method for electromagnetics*, CRC Press, Boca Raton, FL, 1993.
- [12] I. Daubechies, *Ten Lectures on wavelet* (CBMS-NSF Series in Applied Mathematics). Philadelphia, PA: SIAM, 1992.
- [13] S. G. Mallat, *A wavelet tour of signal processing*, Academic Press, 1998.
- [14] G. Deslauriers and S. Dubuc, "Symmetric iterative interpolation processes," *Constr. Approx.*, vol. 5, pp. 49-68, 1989.
- [15] W. Sweldens and R. Piessens, "Wavelet sampling techniques," in *1993 Proceedings of the Statistical Computing Section, American Statistical Association*, San Francisco, pp. 20-29, August 1993
- [16] M. Fujii and W.J.R. Hoefer, "Application of Biorthogonal Interpolating Wavelets to the Galerkin Scheme of Time Dependent Maxwell's Equations," *IEEE Microwave and Wireless Components Letters*, vol.11, no.1, pp.22-24, Jan. 2001.

- [17] Q. Cao, Y. Chen and P. K. A. Wai, "MRTD electromagnetic scattering analysis," *Microwave Opt. Technology. Lett.*, vol, 28, no. 3, pp. 189-195, February 2001.



Dr. Qunsheng Cao is Post-doctoral research associate of AHPCRC at the University of Minnesota in Minneapolis. He received the Bachelor of Science degree in Physics from the University of Huai-Nan Mining, PRC, in 1982, and Ph. D degree from The Hong Kong Polytechnic University, Hong Kong, 2001. In 1989 to 1991, he worked as Visiting Scholar in the Department of Physic, Wuhan University in PRC. In 1994, he became an Associate Professor in Wuhan University of Science and Technology, PRC. From 1996-2001, he became a Research Assistant with The Hong Kong Polytechnic University. From 2001-2002, he became a Research Associate in the Department of Electrical Engineering, University of Illinois at Urbana-Champaign. Since 2002 July, he has worked as a Research Associate in AHPCRC, University of Minnesota in Minneapolis. His current research interests are in computational electromagnetics, wavelet application, parallel technique, using the Time-Domain numerical techniques (FDTD, MRTD and TDFEM) to study microwave devices and scattering applications. He has published 30 international publications in refereed journals and conference symposia. He is a co-author of the book, *Multiresolution Time Domain Scheme for Electromagnetic Engineering* (John Wiley & Sons), a contributor of 2 book chapters.



Dr. Kumar K. Tamma is Professor and Technical Director of Mechanical Engineering and the Army High Performance Computing Research Center (AHPCRC) at the University of Minnesota in Minneapolis. His research

interests include: Computational Mechanics and Multidisciplinary/Multi-scale Physics research developments encompassing Finite-Element Methodology for Interdisciplinary Problem, Computational Algorithms and Numerical Simulation; Fluid/Thermal/Structure Interactions and Thermal Stresses; Manufacturing: Mechanics of Materials and Process Modeling, Residual Stresses, Solidification, Metal Forming; Structural Dynamics, Contact-Impact and Wave Propagation; Solid Mechanics and Large/Aero Space Structures; Microscale/Macroscale/ Nonoscale Heat Transfer and Computational Heat Transfer in Structures and Materials including Composites and Heterogeneous Materials; Computational Methods and Development of Finite Element Algorithms for Large Scale Applications on High Performance Computing Platforms and Parallel Computations; CAD/FEM Interface, Geometric Modeling and Automated/Adaptive Simulation Based Design Techniques. He has authored/co-authored over 160 research articles in various journals and proceedings, and book chapters, and is on the editorial board for ten journals. Professor Tamma has given numerous invited talks, plenary and keynote lectures at various International /National Conference; conducted numerous Workshops/Trainings/Short Courses, and served as Chair/Co-Chair for several conference presentations. Professor Tamma is a member of ASME, AIAA, the International Association for Computational Mechanics, the International Society for Computational and Engineering Science, and the US Association for Computational Mechanics.